Microstructure Evolution and Monomer Partitioning in Reversible Addition−Fragmentation Chain Transfer Microemulsion Polymerization

Jennifer O'Donnell* and Eric W. Kaler

Center for Molecular and Engineering Thermodynamics, Department of Chemical Engineering, University of Delaware, Newark, Delaware 19716

Received March 5, 2008; Revised Manuscript Received June 11, 2008

ABSTRACT: Small-angle neutron scattering (SANS) studies of reversible addition−fragmentation chain transfer (RAFT) microemulsion polymerizations of butyl acrylate and 2-ethylhexyl acrylate with the RAFT agent methyl-2-(*O*-ethylxanthyl)propionate (MOEP) allow the observed rate retardation to be attributed to slow fragmentation of the macro-RAFT radical. Microemulsion polymerization allows the RAFT mechanism to be investigated in the absence of termination reactions so that the cause of the rate retardation frequently observed in both homogeneous and heterogeneous polymerizations may be isolated. However, the concentration of monomer at the locus of polymerization ($C_{mon}^{(part)}$) must be known as a function of conversion before a mechanistic study of the RAFT reaction can be completed. SANS is uniquely capable of probing the evolving microstructure of both the micelles and polymer particles during the polymerization. $C_{mon}^{(part)}$ then can be calculated by combining this microstructural information with material balances on the components of the microemulsion.

Introduction

Reversible addition−fragmentation chain transfer (RAFT) is a robust method for controlling the polymerization of many monomers over a wide range of reaction conditions. However, rate retardation is commonly observed in RAFT polymerizations. In the original RAFT reaction mechanism proposed by Chiefari et al.[1] rate retardation is attributed to slow fragmentation of the macro-RAFT radical (PX•P) during the exchange of radical activity between active (P•) and dormant polymers (PX):

$$P_m^{\bullet} + P_nX \rightleftarrows P_mX^{\bullet}P_n \rightleftarrows P_mX + P_n^{\bullet}$$

High-level ab initio molecular orbital calculations have shown that slow fragmentation of the macro-RAFT radical is in fact a likely source of rate retardation.[2−5] However, experimental evidence of long-lived macro-RAFT radicals has proven inconclusive,[6−10] and this has led to proposed additions to the RAFT reaction mechanism to incorporate either reversible or irreversible termination of the macro-RAFT radical.[10−13] The presence of terminated macro-RAFT radicals also cannot be confirmed experimentally under normal polymerization conditions,[14,15] and therefore, the true source of rate retardation is not yet established.[16] As a result of this mechanistic uncertainty, estimates of the fragmentation rate constant span 8 orders of magnitude.[17,18] The complete scope of the problems that arise due to the mechanistic uncertainties in RAFT polymerizations and a summary of existing experimental and theoretical work have been published by the IUPAC task group "Towards a Holistic Mechanistic Model for RAFT Polymerizations: Dithiobenzoates as Mediating Agents".[16]

Microemulsions provide an ideal medium for studying controlled polymerization mechanisms. In a microemulsion polymerization propagating radicals are segregated into surfactant-stabilized polymer particles, which drastically reduces the probability of biradical termination and, therefore, simplifies the controlled polymerization kinetics. In addition, the Morgan kinetic model[19] for uncontrolled microemulsion polymerization provides a sound basis for examining controlled microemulsion polymerization kinetics. The Morgan model begins with the fundamental rate equation for microemulsion polymerization, which is first order in the concentration of monomer and propagating radicals:

$$\frac{df}{dt} = \frac{k_p C_{mon}^{(part)} N^*}{M_0} \tag{1}$$

k_p is the propagation rate constant, $C_{mon}^{(part)}$ is the concentration of monomer at the locus of polymerization, N^* is the concentration of propagating radicals, and M_0 is the initial concentration of monomer in the microemulsion. Assuming negligible biradical termination and linear monomer partitioning, the rate of conversion of monomer is simply

$$\frac{df}{dt} = \frac{2k_d I_0 k_p C_{mon,0}^{(part)}(1-f)t}{M_0} \tag{2}$$

where $C_{mon,0}^{(part)}$ is the initial concentration of monomer at the locus of polymerization, k_d is the effective dissociation constant of the initiator, and I_0 is the initial initiator concentration. A significant result of this model is the prediction of a rate maximum at 39% conversion independent of the microemulsion composition or rate constants.

RAFT microemulsion polymerizations of butyl acrylate (BA)[20] and 2-ethylhexyl acrylate (EHA)[21] with the chain transfer agent methyl-2-(*O*-ethylxanthyl)propionate (MOEP) (Figure 1) have shown increasing rate retardation as the MOEP/micelle ratio increases. The assumption of negligible biradical termination is valid at the low initiator concentrations used, so this rate retardation seems to indicate the presence of long-lived macro-RAFT radicals. However, the observed rate retardation is accompanied by a shift in the rate maximum from the anticipated value of 39% conversion to ∼20% conversion as the MOEP/micelle ratio increases from 0 to 4.9. Work by deVries et al. has shown that deviations of the location of the rate maximum from the 39% conversion predicted by the Morgan model can be caused by nonlinear monomer partitioning.[22] Nonlinear monomer partitioning could also cause a reduction in the concentration of monomer at the locus of polymerization and explain the observed rate retardation. Therefore, the partitioning

* To whom correspondence should be addressed: Ph +61 2 9351 3535; e-mail odonnell@chem.usyd.edu.au.

10.1021/ma8004923 CCC: $40.75
Published on Web 07/10/2008

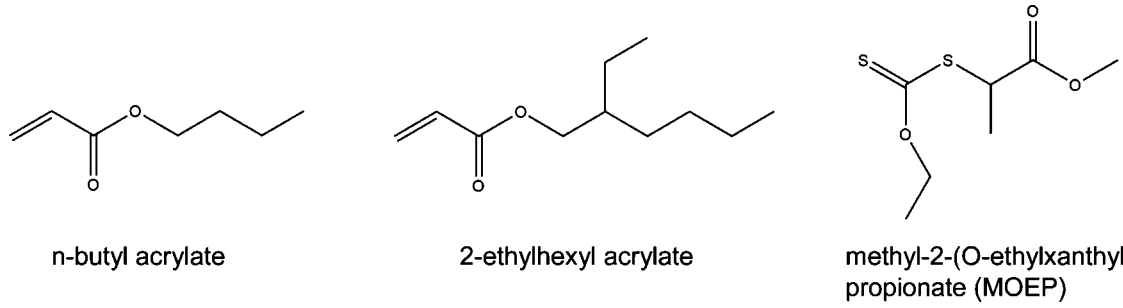

Figure 1. Monomers and chain transfer agent used in this work.

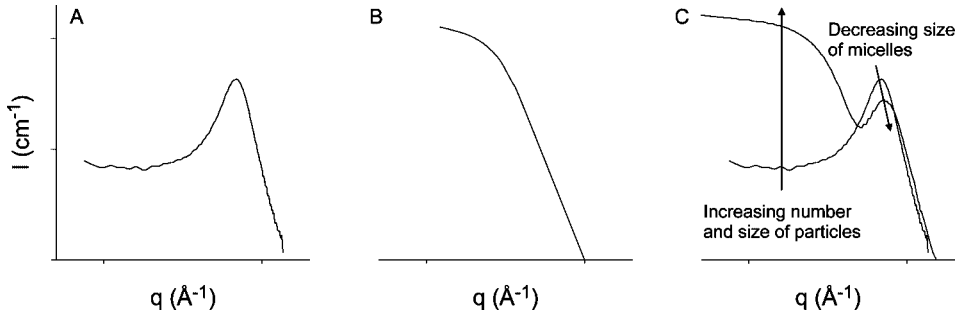

Figure 2. Scattering intensity (I) as a function of the scattering vector (q) for (A) a microemulsion (B) polymer particles (C) polymerizing microemulsion.

of monomer as a function of conversion in the RAFT microemulsion polymerizations of BA and EHA with MOEP must be known before rate retardation can be definitively attributed to long-lived macro-RAFT radicals.

The concentration of monomer at the locus of polymerization can be calculated by coupling mass balances of surfactant, monomer, and polymer with information on the microstructural evolution of the micelles and polymer particles during the polymerization.[23] Small-angle neutron scattering (SANS) is uniquely capable of probing the microstructure of the micelles and polymer particles during microemulsion polymerization without destroying the radical activity. SANS detects the intensity (I) of the scattered neutrons as a function of the momentum change (q) relative to the incident beam. The magnitude of the momentum change, also called the scattering vector, is given by

$$q = \frac{4\pi}{\lambda} \sin\left(\frac{\theta}{2}\right) \tag{3}$$

where λ is the wavelength and θ is the scattering angle. If the scattering material is isotropic and all of the particles in the scattering volume are identical, then the scattering intensity can be written as

$$I(q) = n_p P(q)\, S(q) \tag{4}$$

where n_p is the number density of scattering centers, $P(q)$ is the form factor, and $S(q)$ is the structure factor. $P(q)$ depends on the size and shape of the individual scatters, while $S(q)$ depends on the arrangement of scattering centers, which is described by the three-dimensional Fourier transform of the pair correlation function $g(r)$

$$S(q) = 1 + 4\pi n_p \int_0^\infty [g(r) - 1] \frac{\sin qr}{qr} r^2 \, dr \tag{5}$$

The SANS scattering intensity of polymerizing microemulsions (Figure 2c) has a structure factor peak at intermediate q values (Figure 2a), which is attributed to the micelles, and form factor scattering at low q values (Figure 2b), which is attributed to the polymer particles. A decrease in the micelle structure factor peak intensity and a shift of the peak to higher q values as a function of monomer conversion demonstrates a decrease in intermicellar distance resulting from both increasing micelle number density and decreasing micelle size. As the conversion of monomer increases, the intensity of the low q scattering also increases due to increasing polymer particle size and/or number density.

Experimental Section

Materials. Dodecyltrimethylammonium bromide (DTAB) and didodecyldimethylammonium bromide (DDAB) from TCI America with 99+% purity, the initiator 2,2′-azobis[2-(2-imidazolin-2-yl)propane] dihydrochloride (VA-044) from Wako Pure Chemical Industries, and deuterium oxide from Cambridge Isotopes were used as received. *n*-Butyl acrylate (Aldrich, 99+%) was distilled under vacuum to remove the inhibitor and stored at 2 °C for less than 1 week prior to use. 2-Ethylhexyl acrylate was passed through an inhibitor removal column and stored at 2 °C for less than 1 week prior to use. The RAFT chain transfer agent methyl-2-(*O*-ethylxanthyl)propionate (MOEP) was provided by Rhodia and used as received.

Polymerizations with Small-Angle Neutron Scattering. Microemulsions of *n*-butyl acrylate (BA) in deuterium oxide (D_2O) stabilized by DTAB were prepared at $\alpha = 4.8$, $\gamma = 11.5$, and 45 °C, where $\alpha = \text{mass}_{oil}/(\text{mass}_{oil} + \text{mass}_{D2O}) \times 100$ and $\gamma = \text{mass}_{surfactant}/(\text{mass}_{surfactant} + \text{mass}_{oil} + \text{mass}_{D2O}) \times 100$. A mixed surfactant system of DTAB and DDAB was used to stabilize the 2-ethylhexyl acrylate (EHA) in water microemulsions. The EHA microemulsions were prepared at $\alpha = 3.8$, $\gamma = 11.5$, $\delta = 20.0$, and 45 °C, where $\delta = \text{mass}_{DDAB}/(\text{mass}_{DDAB} + \text{mass}_{DTAB}) \times 100$. The surfactant was added to a 500 mL jacketed glass reactor, and the reactor was purged with nitrogen for 30 min. The pressure in the reactor was maintained at 2 psig during the polymerization. Deuterium oxide was degassed under vacuum, pressurized with nitrogen, and added to the reactor. The temperature of the reactor was increased to the reaction temperature of 45 °C. The monomer and chain transfer agent were mixed, purged with nitrogen, and added to the reactor. Polymerizations of BA were performed at MOEP/micelle ratios of 0.3, 0.6, 1.2, and 4.8, where the concentration of micelles was calculated from the surface area of the surfactant headgroups and the total volume of surfactant and monomer.[21] Polymerizations of EHA were performed at MOEP/

micelles ratios of 0.6, 1.3, 2.4, 3.8, and 4.8. The microemulsion was allowed to equilibrate before the polymerization was initiated by injecting a solution of initiator in deuterium oxide.

Two samples were drawn from the reactor at each sample time. One sample was drawn into a glass vial for gravimetric analysis of the monomer conversion. The gravimetric samples were dried under air flow, washed with acetone to remove excess monomer, and then dried at 50 °C in a vacuum oven overnight. The other sample was drawn directly into a "banjo" cell that was thermostated at the reaction temperature. This sample was immediately placed in the neutron beamline at an intermediate detector distance, which corresponded to $0.01 < q < 0.2$ Å^{-1}, and the scattering intensity was measured for 2 min. The unpolymerized microemulsions and the fully polymerized samples were measured at three detector distances to acquire the scattering intensity over the entire available q range, which is necessary for determining the background scattering. The transmission of the fully polymerized sample was used to correct the samples measured at intermediate conversions.

Quasi-Elastic Light Scattering. Latex solutions were diluted so that the surfactant concentration was 10 times the critical micelle concentration of DTAB (cmc = 16 mM). Quasi-elastic light scattering experiments were performed using a BI9000 digital correlator from Brookhaven Instrument Corp. The scattering angle was fixed at 90°, and samples thermostated at 25 °C were irradiated with 488 nm light produced from a Lexel 2 W argon ion laser. Intensity correlation data were analyzed by the method of cumulants to provide the average decay rate, $\langle\Gamma\rangle = q^2D$, where D is the diffusion coefficient, and the normalized variance $\nu = [(\langle\Gamma^2\rangle - \langle\Gamma\rangle^2)/\langle\Gamma\rangle^2]$. The measured diffusion coefficients were represented in terms of apparent radii by using Stokes' law and assuming the solvent has the viscosity of water.

Results and Discussion

Qualitative Analysis of Small-Angle Neutron Scattering Spectra. The SANS spectra for the RAFT microemulsion polymerizations of butyl acrylate (BA) show a steady decrease in the micelle structure factor peak at intermediate q accompanied by a steady increase of the polymer form factor scattering at low q (Figure 3). The steady shift of the intermediate q peak indicates that monomer is slowly diffusing from the micelles into the polymer particles throughout the polymerization, as opposed to swelling the core of the polymer particles and depleting the micelles early in the polymerization. Therefore, the polymerization is primarily occurring in the corona of monomer and surfactant tails that surrounds the polymeric core of the particles.

The SANS spectra of polymerizing 2-ethylhexyl acrylate (EHA) microemulsions show very different trends than the BA RAFT microemulsion polymerizations. At low MOEP/micelle ratios the structure factor peak at intermediate q increases and shifts to lower q values as the polymerization proceeds (Figure 4). The width of the peak also increases significantly throughout the polymerization. At an MOEP/micelle ratio of 2.4, the intensity of the structure factor peak decreases as a function of conversion, as expected, but the peak shifts to lower q values. Further increasing the MOEP/micelle ratio to 3.8 recovers the typical SANS spectra.

The unusual shift of the structure factor peak in the EHA polymerizations is due to the small size of the EHA polymer particles, as demonstrated by comparing the polymer particle diameters of BA and EHA measured by quasi-elastic light scattering (Figure 5). The BA polymer particles are significantly larger than the unpolymerized micelles, which are less than 5 nm in diameter, so the form factor scattering from the polymer particles is distinct from the structure factor scattering peak of the micelles. However, the hydrodynamic diameter of the EHA polymer particles is ~10 nm, which means that the size distribution of polymer particles overlaps the micelle size. As the MOEP/micelle ratio increases, the size of the EHA polymer particles increases slightly due to coalescence facilitated by increased reaction times, and the anticipated shift of the structure factor peak is recovered. This increase in particle size is not great enough to isolate the structure factor peak from the micelles and calculate the micelle size and number density. Therefore, the scattering from the polymerizing EHA microemulsions cannot be fit, and the quantitative analysis of the SANS spectra presented in the following section focuses only on the BA RAFT microemulsion polymerizations.

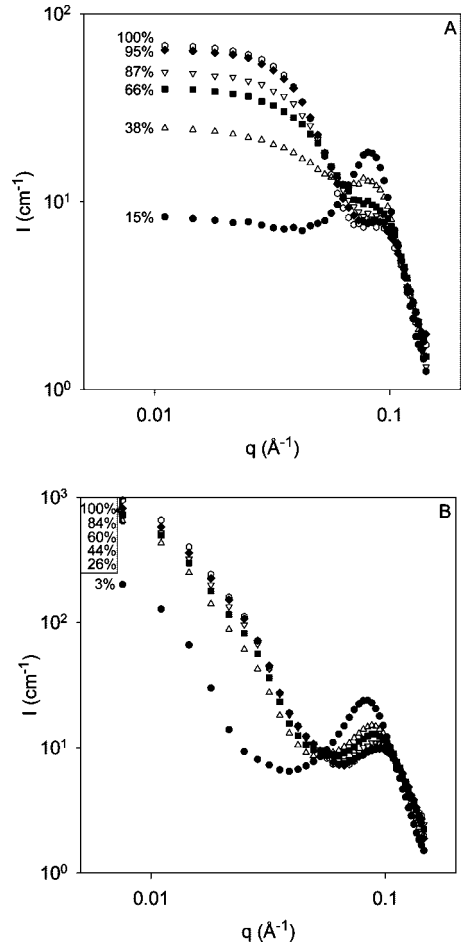

Figure 3. Small-angle neutron scattering intensity (I) as a function of the scattering vector (q) for polymerizing microemulsions of butyl acrylate at MOEP/micelle ratios of (A) 0.3 and (B) 4.9.

Quantitative Analysis of Small-Angle Neutron Scattering Spectra. Previous work by Co and Kaler[23,24] details the application of Vrij's[25] model, which describes the scattering intensity as a function of q for a multicomponent mixture of hard spheres, to polymerizing microemulsions. In this model the micelles are considered to be core−shell prolate ellipsoids where the core is a uniform mixture of monomer and a fraction of the methylene groups from the surfactant tails. The shell is modeled as a uniform mixture of the surfactant headgroups, counterions, water molecules of hydration, and the remaining methylene groups from the surfactant tails. The number of water molecules of hydration for the ammonium headgroups and the bromide counterions were fixed at one and four, respectively, and the fraction of associated counterions was fixed at 0.70 ± 0.02 in accordance with previous work by Lusvardi et al.[26] Intermicellar interactions are approximated by effective hard-sphere excluded-volume interactions. The polymer particles are modeled as spherical polymer cores with an inner shell that is identical to the core of the micelles and an outer shell that is identical to the shell of the micelles.

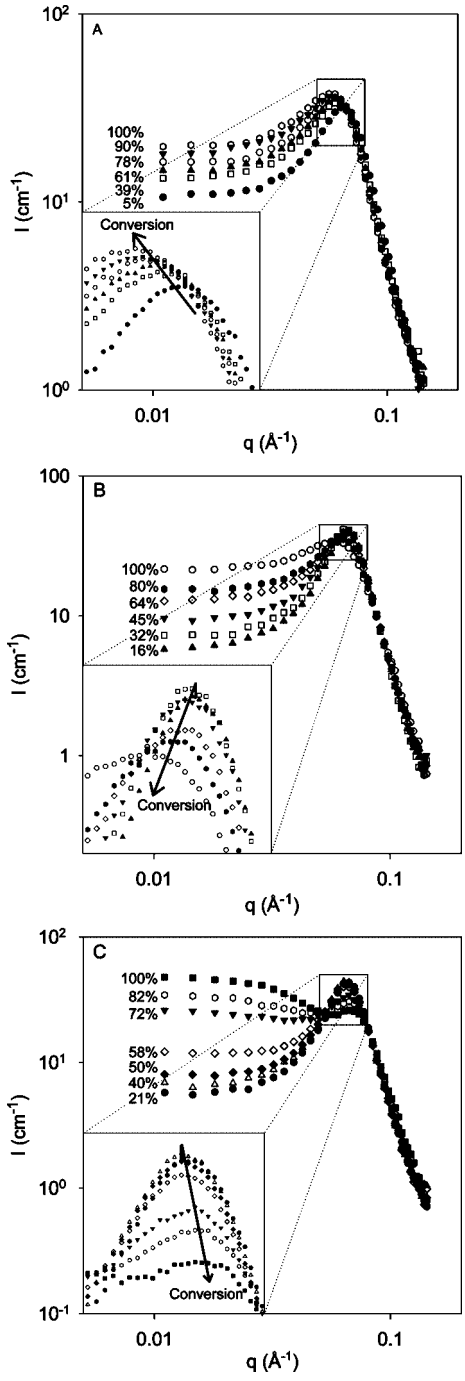

Figure 4. SANS spectra of polymerizing EHA microemulsions at MOEP/micelle ratios of (A) 0.6, (B) 2.4, and (C) 3.8. The insets show the shift of the micelle peak as a function of conversion.

The hydrophobic RAFT agent is assumed to partition into the core of the monomer swollen micelles in the unpolymerized microemulsions. During the polymerization the RAFT agent diffuses into the polymer particles and reacts with propagating polymers to produce radical R groups and dormant polymers. The radical R group initiates a new polymer and is assumed to partition into the core of the polymer particle as that polymer propagates. However, the degree of control imparted to the polymerization[20] necessitates that the RAFT agent cap on the dormant polymer remains in the inner shell of the polymer particle where the polymerization is occurring.

The SANS spectra of unpolymerized BA microemulsions with varying concentrations of MOEP were fit to determine the number of methylene groups in the shell, the aspect ratio of

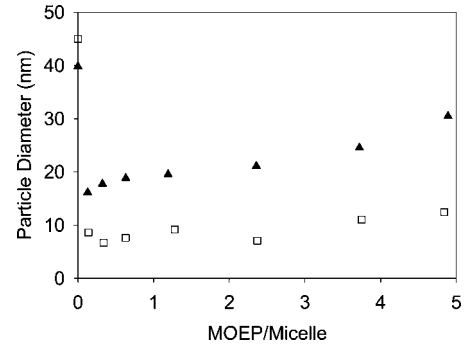

Figure 5. Polymer particle diameter of BA (▲) and EHA (□) calculated by averaging the results of four quasi-elastic light scattering experiments fit with the method of cumulants.

Table 1. Average and Standard Deviation of the SANS Fitting Parameters for Unpolymerized Microemulsions with Varying MOEP/Micelle Ratios

parameter	butyl acrylate with MOEP
number of methylene groups in the shell	2.45 ± 0.20
micelle aspect ratio	2.10 ± 0.20
micelle effective hard-sphere ratio	1.60 ± 0.05

the micelles, and the effective hard-sphere ratio (Table 1). The addition of MOEP did not significantly alter the microstructure of the unpolymerized BA microemulsions. Good agreement is observed between the calculated values for BA/MOEP microemulsions and the values reported by Lusvardi et al. for hexyl methacrylate (HMA) microemulsions with the same surfactant and at similar distances from the phase boundary.[26] The number of methylene groups in the shell is expected to be slightly greater for HMA because the more hydrophobic nature of HMA favors partitioning of the monomer further from the interface.

The scattering spectra of the polymerizing microemulsions were fit with the parameters in Table 1 fixed. The intermediate q region of the scattering intensity, which describes the micelles, was fit to the model first by adjusting only the minor shell radius. As expected, the single micelle volume steadily decreases throughout the polymerization as monomer diffuses from the micelles to the polymer particles (Figure 6). The decrease in micelle size is accompanied by an increase in the micelle number density.

The low q region was then fit by adjusting the mean and standard deviation of the Schultz distribution of polymer particle diameters. Good agreement between the data and the model can be obtained when the polymerizations reach 100% conversion (Figure 7A). However, inaccuracies of up to 5% in measuring the conversion during the polymerization result in deviations between the model and the data at intermediate conversions (Figure 7B). The most significant deviations between the model

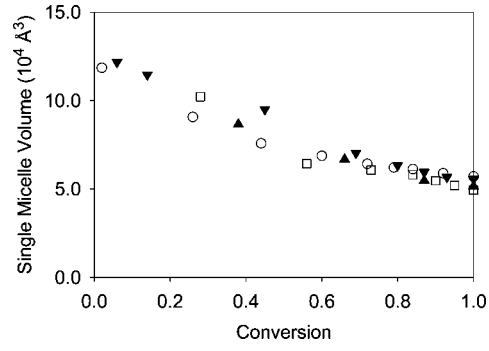

Figure 6. Volume of BA swollen DTAB micelles as a function of conversion at MOEP/micelle ratios of 0.3 (▲), 0.6 (□), 1.2 (▼), and 4.9 (○).

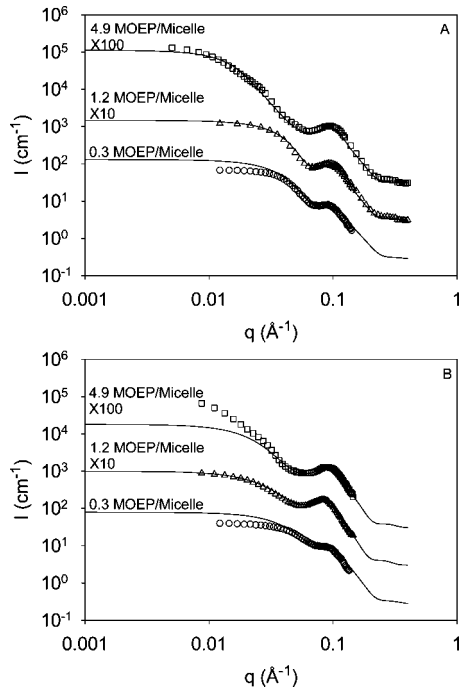

Figure 7. SANS spectra of BA polymerizations at (A) 100% conversion and (B) ~45% conversion. The lines are the model fits.

Table 2. Polymer Particle Diameters Calculated by SANS and QLS

MOEP/micelle	SANS particle diameter (nm)	QLS particle diameter (nm)
0.3	14.9	17.8
0.6	14.0	18.8
1.2	14.0	19.5
4.9	29.5	30.5

and the data are found for the polymerizations at an MOEP/micelle ratio of 4.9. At this MOEP/micelle ratio, the model predicts significantly lower scattering intensities from the polymer particles. The poly(butyl acrylate) particle diameter increases as the MOEP/micelle ratio increases because coalescence of the particles is facilitated by the increased polymerization time[20] (Figure 5). Therefore, the Schultz distribution may not accurately represent the population of poly(butyl acrylate) particles at high MOEP/micelle ratios. A low concentration of large polymer particles may cause a significant increase in the scattering intensity at low q.

The z-average diameters of the fully polymerized particles calculated from the SANS spectra fits are in good agreement with the particle sizes measured by quasi-elastic light scattering (QLS) (Table 2).

The concentration of monomer at the locus of polymerization ($C_{mon}^{(part)}$) was calculated from the microstructure of the polymerizing microemulsions and mass balances of the surfactant, monomer, and polymer, as described by Co and Kaler.[23] The decrease in $C_{mon}^{(part)}$ as a function of conversion shows a slight positive deviation from linearity at all MOEP/micelle ratios (Figure 8). This positive deviation from linearity indicates that the incorporation of the RAFT agent MOEP allows for some additional swelling of the polymer particles.

The positive deviation of the monomer concentration from the predicted value shows that monomer partitioning does not cause the observed rate retardation. Therefore, because biradical termination reactions are negligible in microemulsion polymerizations at the initiator concentrations used,[19] these results allow rate retardation to be definitively attributed to slow fragmentation of the macro-RAFT radicals during the polymerization. Additionally, the assumptions of the Morgan model for uncontrolled microemulsion polymerization kinetics have been validated for RAFT microemulsion polymerization kinetics. Therefore, the Morgan model can be used to further explore the RAFT reaction mechanism.

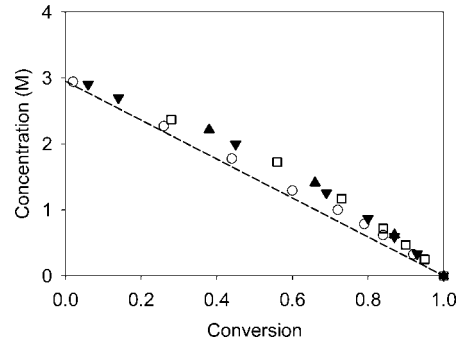

Figure 8. Concentration of BA at the locus of polymerization as a function of conversion at MOEP/micelle ratios of 0.3 (▲), 0.6 (□), 1.2 (▼), and 4.9 (○). The linear decrease is predicted from the concentration of monomer in the unpolymerized micelles.

Conclusions

Small-angle neutron scattering of polymerizing microemulsions captures the microstructural evolution of the micelles and polymer particles. When the polymer particles are sufficiently large relative to the micelles, the SANS spectra shows structure factor scattering from the micelles at intermediate q values and form factor scattering from the polymer particles at low q. However, when the polymer particles remain approximately the same size as the micelles, the scattering from the micelles and polymer particles cannot be isolated.

The concentration of monomer at the locus of polymerization during the RAFT microemulsion polymerization of butyl acrylate decreases nearly linearly with conversion. A slight positive deviation from linearity indicates that monomer partitioning does not cause the observed rate retardation in RAFT microemulsion polymerization. Therefore, the SANS results allow rate retardation during RAFT microemulsion polymerizations to be definitively attributed to slow fragmentation of the macro-RAFT radical. This is consistent with the original RAFT reaction mechanism proposed by Chiefari et al.[1]

Acknowledgment. We acknowledge the support of the National Institute of Standards and Technology, U.S. Department of Commerce, in providing the neutron facilities used in this work. This work utilized facilities supported in part by the National Science Foundation under Agreement DMR-0454672.

References and Notes

(1) Chiefari, J.; Chong, Y. K.; Ercole, F.; Krstina, J.; Jeffery, J.; Le, T. P. T.; Mayadunne, R. T. A.; Meijs, G. F.; Moad, C. L.; Moad, G.; Rizzardo, E.; Thang, S. H. *Macromolecules* **1998**, *31*, 5559.
(2) Coote, M. L.; Radom, L. *J. Am. Chem. Soc.* **2003**, *125*, 1490.
(3) Feldermann, A.; Coote, M. L.; Stenzel, M. H.; Davis, T. P.; Barner-Kowollik, C. *J. Am. Chem. Soc.* **2004**, *126*, 15915.
(4) Coote, M. L. *Macromolecules* **2004**, *37*, 5023.
(5) Coote, M. L.; Izgorodina, E. I.; Krenske, E. H.; Busch, M.; Barner-Kowollik, C. *Macromol. Rapid Commun.* **2006**, *27*, 1015.
(6) Calitz, F. M.; Tonge, M. P.; Sanderson, R. D. *Macromolecules* **2003**, *36*, 5.
(7) Buback, M.; Hesse, P.; Junkers, T.; Vana, P. *Macromol. Rapid Commun.* **2006**, *27*, 182.
(8) Barner-Kowollik, C.; Quinn, J. F.; Nguyen, T. L. U.; Heuts, J. P. A.; Davis, T. P. *Macromolecules* **2001**, *34*, 7849.
(9) Hawthorne, D. G.; Moad, G.; Rizzardo, E.; Thang, S. H. *Macromolecules* **1999**, *32*, 5457.
(10) Kwak, Y.; Goto, A.; Tsujii, Y.; Murata, Y.; Komatsu, K.; Fukuda, T. *Macromolecules* **2002**, *35*, 3026.
(11) Buback, M.; Vana, P. *Macromol. Rapid Commun.* **2006**, *27*, 1299.

(12) Kwak, Y.; Goto, A.; Fukuda, T. *Macromolecules* **2004**, *37*, 1219.
(13) Monteiro, M. J.; de Brouwer, H. *Macromolecules* **2001**, *34*, 349.
(14) Ah Toy, A.; Vana, P.; Davis, T. P.; Barner-Kowollik, C. *Macromolecules* **2004**, *37*, 744.
(15) Feldermann, A.; Toy, A. A.; Davis, T. P.; Stenzel, M. H.; Bamer-Kowollik, C. *Polymer* **2005**, *46*, 8448.
(16) Barner-Kowollik, C.; Buback, M.; Charleux, B.; Coote, M. L.; Drache, M.; Fukuda, T.; Goto, A.; Klumperman, B.; Lowe, A. B.; McLeary, J. B.; Moad, C. L.; Monteiro, M. J.; Sanderson, R. D.; Tonge, M. P.; Vana, P. *J. Polym. Sci., Part A: Polym. Chem.* **2006**, *44*, 5809.
(17) Barner-Kowollik, C.; Quinn, J. F.; Morsley, D. R.; Davis, T. P. *J. Polym. Sci., Part A: Polym. Chem.* **2001**, *39*, 1353.
(18) Wang, A. R.; Zhu, S. P. *J. Polym. Sci., Part A: Polym. Chem.* **2003**, *41*, 1553.
(19) Morgan, J. D.; Lusvardi, K. M.; Kaler, E. W. *Macromolecules* **1997**, *30*, 1897.
(20) O'Donnell, J.; Kaler, E. W. *Macromolecules*, submitted.
(21) O'Donnell, J. Reversible Addition-Fragmentation Chain Transfer Polymerization in Microemulsions. Ph.D. Thesis, Chemical Engineering, University of Delaware, **2007**.
(22) de Vries, R.; Co, C. C.; Kaler, E. W. *Macromolecules* **2001**, *34*, 3233.
(23) Co, C. C.; Kaler, E. W. *Macromolecules* **1998**, *31*, 3203.
(24) Co, C. C.; de Vries, R.; Kaler, E. W. *Macromolecules* **2001**, *34*, 3224.
(25) Vrij, A. *J. Chem. Phys.* **1979**, *71*, 3267.
(26) Lusvardi, K. M.; Full, A. P.; Kaler, E. W. *Langmuir* **1995**, *11*, 487.

MA8004923